Inorg. Chem. **2004**, *43*, 1969–1975

Inter-String Arrays of Bimetallic Assemblies with Alternative Cu^{2+}–Cl–Cu^{2+} and Cu–NC–M (M = Co^{3+}, Fe^{+3}, Cr^{+3}) Bridges: Syntheses, Crystal Structure, and Magnetic Properties

Manas K. Saha,[†] Francesc Lloret,[‡] and Ivan Bernal*,[†]

Department of Chemistry, University of Houston, Texas 77204, and Department de Química Inorgánica, Facultat de Química de la Universitat de València, Dr. Moliner 50, 46100 Burjassot (València), Spain

Received July 29, 2003

Three bimetallic assemblies with alternate homometallic bridges through chloride ligands and heterometallic bridges through cyanide ligands of formula $[(323)_2Cu_2(Cl)M(CN)_6]_n \cdot 2n(H_2O)$, where 323 = *N*,*N*′-bis(3-aminopropyl)-ethylenediamine and M = Co^{3+} for **1**, Fe^{3+} for **2**, and Cr^{3+} for **3**, were synthesized. They have been characterized structurally, analytically, spectroscopically, and magnetically. All three assemblies crystallize in the monoclinic system in the same space group $P2_1/n$, with a = 11.642(2) Å, b = 10.285(3) Å, c = 13.622(2) Å, β = 95.69(3)°, V = 1623.1(6) Å^3, and Z = 4 for **1**; a = 11.681(4) Å, b = 10.315(3) Å, c = 13.567(5) Å, β = 95.62(3)°, V = 1626.8(9) Å^3, Z = 4 for **2**, and a = 11.782(4) Å, b = 10.386(2) Å, c = 13.755(4) Å, β = 95.51(3)°, V = 1657.4(8) Å^3, Z = 4 for **3**. Crystal structure analyses reveal that one-dimensional zigzag chains propagate in two different crystallographic directions (*a* and *b*) which are held together during the course of their propagation. All three assemblies have a homometallic Cu–Cl–Cu core in common. Assembly **1** exhibits metamagnetic behavior and shows weak antiferromagnetic interactions between Cu^{2+} paramagnetic centers, through the chloride bridges. The Neel temperature, T_N, is 3.5 K, and the critical field is 4 T. In the presence of a magnetic field larger than 4 T, the local spin doublets of Cu^{2+} in the assembly **1** remain in parallel arrangements. Assemblies **2** and **3** may be described as an alternative repetition of the antiferromagnetically coupled Cu–Cl–Cu fragment and ferromagnetically coupled Cu–CN–Fe^{3+}/Cr^{3+}fragment. The overall magnetic character of the strings in assemblies **2** and **3** are antiferromagnetic. Ferromagnetic interaction evidenced by the (Cu–CN–Fe^{3+}/Cr^{3+}) fragment was masked by the antiferromagnetic interaction between the Cu^{2+} centers through the chloride bridge. The magnetic properties agree well with those expected for two [323 Cu^{2+}] and a $[Fe(CN)]^{3+}$ unit with spin–orbit coupling effect of the low-spin iron(III) ions for **2** and for two [323 Cu^{2+}] and a $[Cr(CN)]^{3+}$ unit for **3**. In aqueous solution, trinuclear $[(323)_2Cu_2M(CN)_6]^+$ and dinuclear $[(323)CuM(CN)_6]^-$ species were observed.

Introduction

Hexacyanometalates are building blocks that can be utilized to construct magnetically coupled systems, while researchers are hoping to discover molecular-based magnets.[1] When hexacyanometalates react with simple metal ions, they give the Prusian blue analogues.[2] Instead of simple ions, when metal complexes with vacant coordination sites are allowed to react, hexacyanometalate ions adopt different bridging modes ranging from η^1 to η^6, to form assemblies.[3] It is becoming clear that transition metal based assembly processes that utilize the hexacyanometalates, as bridging ligands for propagating the coordinate geometries of the

* To whom correspondence should be addressed. E-mail: ibernal@uh.edu.
[†] University of Houston.
[‡] Facultat de Química de la Universitat de València.

(1) (a) Kahn, O. In *Molecular Magnetism*; VCH: Weinheim, Germany, 1993. (b) Gatteschi, D. *Adv. Mater.* **1994**, *6*, 635. (c) Kahn, O. *Advances in Inorganic Chemistry*; Academic Press. Inc.: San Diego, CA, 1995; Vol. 43. (d) Gadet, V.; Bujoli-Doeuff, M.; Force, L.; Verdaguer, M.; El Malkhi, K.; Deroy, A.; Besse, J. P.; Chappert, C.; Veillet, P.; Renald, J. P.; Beauvillian, P. *Magnetic Molecular Materials*; Gatteschi, D., Kahn, O., Miller, J. S., Palacio, F., Eds.; NATO ASI Series E; Kluewer Academic: Dordrecht, The Netherlands, 1991; Vol. 198, p 281. (e) Klenze, H.; Kanellalopulos, B.; Tragester, G.; Eysel, H. *J. Chem. Phys.* **1980**, *72*, 5817. (f) Gadet, V.; Mallah, T.; Castro, I.; T.; Verdaguer, M. *J. Am. Chem. Soc.* **1992**, *114*, 9213. (g) Mallah, T.; Thiebaut, S.; Verdaguer, M.; Veillet, P. *Science* **1993**, *262*, 1554. (h) Entley, W. R.; Girolami, G. S. *Inorg. Chem.* **1994**, *33*, 5165.

10.1021/ic034897n CCC: $27.50
Published on Web 02/21/2004

metals, can lead to novel structural features and physicochemical processes.[1−4]

In this context, one-dimensional, two-dimensional, and three-dimensional structures have attracted interest owing to their ability to form various classes of networks. These systems are constructed by the repetition of two different metal centers bridged through cyanide linkages. Though there is often extreme difficulty in growing crystals of these cyanide complexes, advancement has been achieved in this area. Despite these significant recent advancements, there is little effort to construct assemblies that involve a second bridging agent along with the cyanometalate linkage. The uses of multibridging agents are of particular interest as the combination of two different interacting pathways may frequently constitute very promising molecular magnets.[5] The structural and magnetic characteristics of assemblies containing cyanometalate and a second bridging agent remain relatively undeveloped. A few such systems are reported[6a] and were structurally characterized, but in all cases, the metal centers in the cyanometalate core are magnetically silent; thus, from a magnetic point of view, they are, essentially, dimeric systems. Very recently, a 2-D cyano- and oxamidato-bridged Cr(III)−Cu(II)−Gd(III) system,[6b] a Mn(II)−Fe(III)[6c] system, and a mixed valence Ru−Fe(III)[6d] system were reported, which are the only examples having more than one magnetic center containing cyanometalate along with a second bridging ligand.

In this study, renewed efforts have been made to construct bimetallic assemblies propagating through two different types of bridging ligands simultaneously, repeated in a periodic fashion. The assemblies consist of homometallic Cu−Cl−Cu and heterometallic Cu−CN−M bridges, that can be rationally prepared by the reaction of $[Cu(323)Cl]Cl\cdot H_2O$ and $K_3[M(CN)_6]$ (M = Co, Fe, and Cr) in a 2:1 molar stoichiometry. Analogous assemblies $[(323)_2Cu_2(Cl)Co(CN)_6]_n\cdot 2n(H_2O)$ (**1**), $[(323)_2Cu_2(Cl)Fe(CN)_6]_n\cdot 2n(H_2O)$ (**2**), and $[(323)_2Cu_2(Cl)Cr(CN)_6]_n\cdot 2n(H_2O)$ (**3**) have been obtained which are isomorphous and isostructural, as evidenced by X-ray crystallography. The zigzag chain [Cu−Cl−Cu−NC−M] propagates in different directions, forming a supramolecular network. The cryomagnetic properties of **1**−**3** were studied in the temperature range 1.5−290 K and are discussed from the viewpoint of the different electronic configuration of the metal ions, and their orbital and geometric consideration.

Experimental Section

The component complex $[(323)CuCl]Cl\cdot H_2O$ was prepared by the literature method.[7] The salts $K_3[M(CN)_6]$ (M = Co, Fe and Cr) were purchased from Aldrich Chemical Co., were of reagent grade, and were used as such.

$[(323)_2Cu_2(Cl)Co(CN)_6]_n\cdot 2n(H_2O)$ (1). $[(323)CuCl]Cl\cdot H_2O$ (0.32 g (1 mmol)) was dissolved in 40 cm^3 of water. To this solution was added an aqueous solution (30 cm^3) of $K_3[Co(CN)_6]$ (0.166 g, 0.5 mmol) at room temperature. The resulting solution was allowed to stand overnight to form blue, block-shaped crystals. They were collected by suction filtration. The yield was ca. 80%. All the operations were carried out in the dark to avoid the decomposition of $K_3[Co(CN)_6]$. Anal. Calcd for $C_{22}H_{48}ClCu_2CoN_{14}O_2$: C = 34.67, H = 6.35, N= 25.73, Cl = 4.65. Found: C = 34.78, H = 6.46, N = 25.28, Cl =4.58.

$[(323)_2Cu_2(Cl)Fe(CN)_6]_n\cdot 2n(H_2O)$ (2). This compound was prepared as brown crystals in a procedure similar to that for **1**, except for the use of $K_3[Fe(CN)_6]$ instead of $K_3[Co(CN)_6]$. Anal. Calcd for $C_{22}H_{48}ClCu_2FeN_{14}O_2$: C = 34.81, H = 6.37, N = 25.83; Cl =4.67. Found: C = 34.42, H = 6.31, N = 26.02, Cl = 4.72.

$[(323)_2Cu_2(Cl)Cr(CN)_6]_n\cdot 2n(H_2O)$ (3). It was prepared as blue crystals in a procedure similar to that for **1**, except for the use of $K_3[Cr(CN)_6]$ instead of $K_3[Co(CN)_6]$. Anal. Calcd for $C_{22}H_{48}ClCu_2CrN_{14}O_2$: C = 34.99, H = 6.41, N = 25.96, Cl = 4.69. Found: C = 34.87, H = 6.48, N = 25.43, Cl = 4.77.

Crystal Structure Determination. Suitable crystals of **1** (block, blue, dimensions 0.8 × 0.6 × 0.5 mm^3), **2** (block, brown, dimensions 0.8 × 0.7 × 0.6 mm^3), and **3** (block, blue, dimensions 0.8 × 0.7 × 0.7 mm^3) were used for the structure determination. X-ray data were collected using an Enraf Nonius CAD-4 diffractometer with graphite-monochromatized Mo Kα radiation (λ = 0.71073) by the $\omega-2\theta$ scan mode in the range $0° < 2\theta < 56°$, at room temperature for all three crystals. Unit cell parameters were determined on the basis of 25 reflections within the range $9° < 2\theta < 20°$. During data collection, the intensity of three standard reflections, monitored every 3000 s of X-ray exposure time, showed

(2) (a) Kahn, O. *Nature* **1995**, *378*, 667. (b) Verdaguer, M. *Science* **1996**, *272*, 698. (c) Entley, W. R.; Girolami, G. S. *Science* **1995**, *268*, 397. (d) Dunbar, K. R.; Heintz, R. A. *Progress in Inorganic Chemistry*; John Wiley & Sons: New York, 1997; Vol. 45, p 283. (e) Sato, O.; Iyoda, T.; Fujishima, A.; Hashimoto, K. *Science* **1996**, *271*, 49. (f) Sato, O.; Iyoda, T.; Fujishima, A.; Hashimoto, K. *Science* **1996**, *272*, 704. (g) Herren, F.; Fischer, P.; Ludi, A.; Hälg, W. *Inorg. Chem.* **1980**, *19*, 956.

(3) (a) Parker, R. J.; Spiccia, L.; Batten, S. R.; Cashion, J. D.; Fallon, G. D. *Inorg. Chem.* **2001**, *40*, 4696. (b) Salah El Fallah, M.; Ribas, J.; Solans, X.; Font-Bardia, M. *J. Chem. Soc., Dalton Trans.* **2001**, 247. (c) Mondal, N.; Saha, M. K.; Bag, B.; Mitra, S.; Gramlich, V.; Ribas, J.; El Fallah, M. S. *J. Chem. Soc., Dalton Trans.* **2000**, 1601. (d) Mondal, N.; Saha, M. K.; Mitra, S.; Gramlich, V.; Ribas, J.; Salah El Fallah, M. *Polyhedron* **2000**, 1601. (e) Re, N.; Gallo, E.; Floriani, C.; Miyasaka, H.; Matsumoto, N. *Inorg. Chem.* **1996**, *35*, 5964. (f) Re, N.; Gallo, E.; Floriani, C.; Miyasaka, H.; Matsumoto, N. *Inorg. Chem.* **1995**, *35*, 6004. (g) Miyasaka, H.; Matsumoto, N.; Ōkawa, H.; Re, N.; Gallo, E.; Floriani, C. *Angew. Chem., Int. Ed. Engl.* **1995**, *34*, 1446. (h) Miyasaka, H.; Matsumoto, N.; Ōkawa, H.; Re, N.; Gallo, E.; Floriani, C. *J. Am. Chem. Soc.* **1996**, *118*, 981. (i) Ohba, M.; Ōkawa, H. *Mol. Cryst. Liq. Cryst.* **1996**, *286*, 101. (j) Ōkawa, H.; Obha, M. In *Molecule-Based Magnetic Material: Theory, Techniques and Application*; Turnbull, M. M., Sugimoto, T., Thompson, L. K., Eds.; ACS Symposium Series 644; American Chemical Society: Washington, DC, 1996; p 319.

(4) (a) Colacio, E.; Ghazi, M.; Stoecki-Evans, H.; Lloret F.; Moreno, J. M.; Pérez, C. *Inorg. Chem.* **2001**, *40*, 4876. (b) Kou, H.-Z.; Gao, S.; Ma, B.-Q.; Liao, D.-Z. *J. Chem. Soc., Chem. Commun.* **2000**, 1309. (c) Fu, D. G.; Chen, J.; Tan, X. S.; Jiang, L. J.; Zhang, S. W.; Zheng, P. J.; Tang, W. X. *Inorg. Chem.* **1997**, *36*, 220. (d) Scott, M. J.; Lee, S. C.; Holm, R. H. *Inorg. Chem.* **1994**, *33*, 4561. (e) Gardner, M. T.; Deinum, G.; Kim, Y.; Babcock, G. T.; Scott, M. J.; Holm, R. H. *Inorg. Chem.* **1996**, *35*, 6878.

(5) Konar, S.; Mukherjee, P. S.; Zangrando, E.; Lloret, F.; Chaudhuri, N. R. *Angew. Chem., Int. Ed.* **2002**, *41*, 1561.

(6) (a) Mukherjee, P. S.; Maji, T. K.; Mallah, T.; Zangrando, E.; Randaccio, L.; Ray Chaudhuri, N. *Inorg. Chim. Acta* **2001**, *315*, 249. Cheng, Z. N.; Wang, J. L.; Qiu, J.; Miao, F. M.; Tang, W. X. *Inorg. Chem.* **1995**, *34*, 2255. Niel, V.; Munoz, M. C.; Gaspar, A. B.; Galet, A.; Levchenko, G.; Real, J. A. *Chem.—Eur. J.* **2002**, *8*, 2446. Herrera, J. M.; Amentano, D.; de Munno, G.; Lloret, F.; Julve, M.; Verdaguer. *New J. Chem.* **2003**, *27*, 18. (b) Kou, H.-Z.; Zhou, B. C.; Gao, S.; Wang, R.-J. *Angew. Chem., Int. Ed.* **2003**, *42*, 3288. (c) Toma, L. M.; Lescouezec, R.; Toma, L. D.; Lloret, F.; Julve, M.; Vaissemann, J.; Andruh, M. *J. Chem. Soc., Dalton. Trans.* **2002**, 3171. (d) Yoshioka, D.; Mikuriya, M.; Handa, M. *Chem. Lett.* **2002**, 1044.

(7) Hedwig, G. R.; Love, J. L.; Powell, H. K. J. *Aust. J. Chem.* **1970**, *23*, 981.

Table 1. Crystallographic Data for Complexes **1**, **2**, and **3**

	1	**2**	**3**
formula	$C_{11}H_{24}Cl_{0.5}Co_{0.5}CuN_7O$	$C_{11}H_{24}Cl_{0.5}Fe_{0.5}CuN_7O$	$C_{11}H_{24}Cl_{0.5}Cr_{0.5}CuN_7O$
fw	381.1	379.56	377.64
space group	$P2_1/n$	$P2_1/n$	$P2_1/n$
a (Å)	11.642(2)	11.681(2)	11.782(4)
b (Å)	10.285(3)	10.315(3)	10.386(2)
c (Å)	13.622(2)	13.567(5)	13.755(4)
β (deg)	95.69(3)	95.62(3)	95.51(3)
V (Å^3)	1623.1(6)	1626.8(9)	1675.4(8)
Z	4	4	4
T (K)	293(2)	293(2)	293(2)
λ(Mo Kα Å)	0.71073	0.71073	0.71073
ρ	1.56	1.55	1.497
R1	0.0527	0.0396	0.0445
wR2	0.1258	0.1005	0.1124

no significant decay. The data were processed using the WinGx[8] package of programs, and an empirical absorption correction was employed for all the crystals. The structures were solved by direct methods in SIR-92[9] and SHELXS-86[10] and refined by full-matrix least-squares, based on F^2, using SHELXL-97.[11] All non-H atoms refined anisotropically by unit-weighted full-matrix least-squares methods. Hydrogen atoms were included at calculated positions and refined in the riding mode, except those for water molecules that were located on residual density maps. Their positions were then fixed and refined in a riding mode. For **1**, convergence was reached at a final R1 = 0.0527 [for $I > 2\sigma(I)$], wR2 = 0.1559 (for all data), and 194 parameters, with allowance for the thermal anisotropy for all non-hydrogen atoms. The weighting scheme employed was $w = 1/[\sigma^2(F_o^2 + (0.0328P)^2 + 10.3085P]$ where $P = (|F_o|^2 + 2|F_c^2|)/3$, and the goodness-of-fit on F^2 was 1.097 for all observed reflections. For **2**, convergence was reached at a final R1 = 0.0396 [for $I > 2\sigma(I)$], wR2 = 0.1131 (for all data), and 193 parameters, with allowance for the thermal anisotropy for all non-hydrogen atoms. The weighting scheme employed was $w = 1/[\sigma^2(F_o^2 + (0.0696P)^2 + 1.5466P]$ where $P = (|F_o|^2 + 2|F_c^2|)/3$ and the goodness of fit on F^2 was 0.956 for all observed reflections. For **3**, convergence was reached at a final R1 = 0.0445 [for $I > 2\sigma(I)$], wR2 = 0.1343 (for all data), and 193 parameters, with allowance for the thermal anisotropy for all non-hydrogen atoms. The weighting scheme employed was $w = 1/[\sigma^2(F_o^2 + (0.0653P)^2 + 1.2478P]$ where $P = (|F_o|^2 + 2|F_c^2|)/3$ and the goodness-of-fit on F^2 was 1.030 for all observed reflections. The water molecules of crystallization showed high thermal parameters. Crystal data and details on the data collection and refinement are summarized in Table 1.

Physical Measurements. Elemental analyses of carbon, hydrogen, nitrogen, and chlorine were obtained from Galbraith Analytical Laboratories, 2323 Sycamore Drive, Knoxville, TN 37921-1750. Infrared spectra were measured on a Perkin-Elmer 983 G spectrophotometer using KBr pellets. Electron spray mass spectra in aqueous solution were recorded with an LCQ DECA XP mass spectrometer. Electronic spectra were recorded in aqueous solutions on a Simadzu model MPS-2000 multipurpose spectrophotometer. Magnetic susceptibility and magnetization measurements were performed on polycrystalline samples of **1**−**3** with a Quantum Design SQUID susceptometer covering the 1.9−300 K temperature range and using applied magnetic fields ranging from 100 Oe to 5 T. The susceptometer was calibrated with $(NH_4)_2Mn(SO_4)_2 \cdot 12H_2O$. The experimental susceptibility data of **1**−**3** were corrected for the diamagnetism estimated from Pascal's constants.[12]

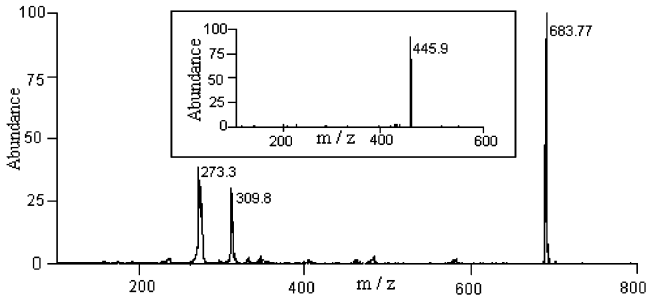

Figure 1. The ESI-MS for assembly **3**. The inset presents the spectra for anionic species.

Result and Discussion

General Properties. All three assemblies show very similar IR spectra. A very strong band at ∼3380 cm^{-1} indicates the presence of water molecules. The hexacyanide ligand band ν(C−N) appears at 2138, 2123, and 2136 cm^{-1} for **1**, **2**, and **3**, respectively. A wide range between ∼3250−3140 cm^{-1} is due to ν(N−H), and the bands in ∼2950−2875 cm^{-1} are assigned to ν(C−H). Finally, characteristic bands for the 323 ligand at ∼1463−1140 cm^{-1} were observed.[13]

All the species are stable in air and insoluble in almost all organic and inorganic solvents, except that they dissolve moderately well in hot water. However, when allowed for a long period (45 min), they dissolve in water at room temperature. All the three assemblies produce trimeric $[(323)_2Cu_2M(CN)_6]^+$, dimeric $[(323)CuM(CN)_6]^-$, and monomeric $[(323)Cu(Cl)]^+$and $[(323)Cu(Cl)_2]$ species in aqueous solution as evidenced by the ES-MS spectroscopy. In Figure 1, we show the spectra for the chromium(III) analogue **3**, as a representative, where the existence of the $[(323)_2Cu_2Cr(CN)_6]^+$ and $[(323)Cu(Cl)]^+$ moieties was indicated by the peaks at m/z 683.7 and 273.3, respectively, and for neutral $[(323)Cu(Cl)_2]$ species, at $(M + H^+)/z$ 309.7. The inset in Figure 1 shows the spectra for the anionic dinuclear moiety $[(323)CuCr(CN)_6]^-$ with a peak at m/z 445.9. Spectra for **1** and **2** show peaks for $[(323)Cu(Cl)]^+$ and $[(323)Cu(Cl)_2]$ at the same position. The peaks for trinuclear moieties $[(323)_2Cu_2Co(CN)_6]^+$ and $[(323)_2Cu_2Fe(CN)_6]^+$ were observed at m/z 690.7 and 687.6, respectively, and at m/z 452.9 and 449.8 for the anionic dinuclear unit $[(323)CuCo(CN)_6]^-$ and $[(323)CuFe(CN)_6]^-$, respectively.

The electronic spectra of **1** show two very strong absorptions at 240 and 270 nm, one strong absorption at 318 nm, and one moderately strong adsorption at 540 nm. The band at 318 nm can be assigned to the d−d transition band ($^1T_{1g} \rightarrow {}^1A_{1g}$)[14] of $[Co(CN)_6]^{3+}$, and the visible band at 540 nm is

(8) Farrugia, L. *J. Appl. Crystallogr.* **1999**, *32*, 837.
(9) Altomare, A.; Cascarano, G.; Giacovazzo, C.; Gualardi, A. *J. Appl. Crystallogr.* **1993**, *26*, 343.
(10) Sheldrick G. M. *SHELXS-86: Program for the Solution of Crystals Structures*; University of Göttingen: Göttingen, Germany, 1986.
(11) S*HELXL-97: Program for the Refinement of Crystal Structures*; University of Göttingen: Göttingen, Germany, 1997.
(12) Figgis, B. N.; Lewis, J. *Technique of Inorganic Chemistry*; Jonassen, H. B., Weissberger, A., Eds.; John Wiley and Sons: New York, 1965; Vol. IV, p 137.
(13) Nakamoto, K. *Infrared and Raman Spectra of Inorganic and Coordination Compounds*, 4th ed.; Wiley-Interscience: New York, 1978; Part B.

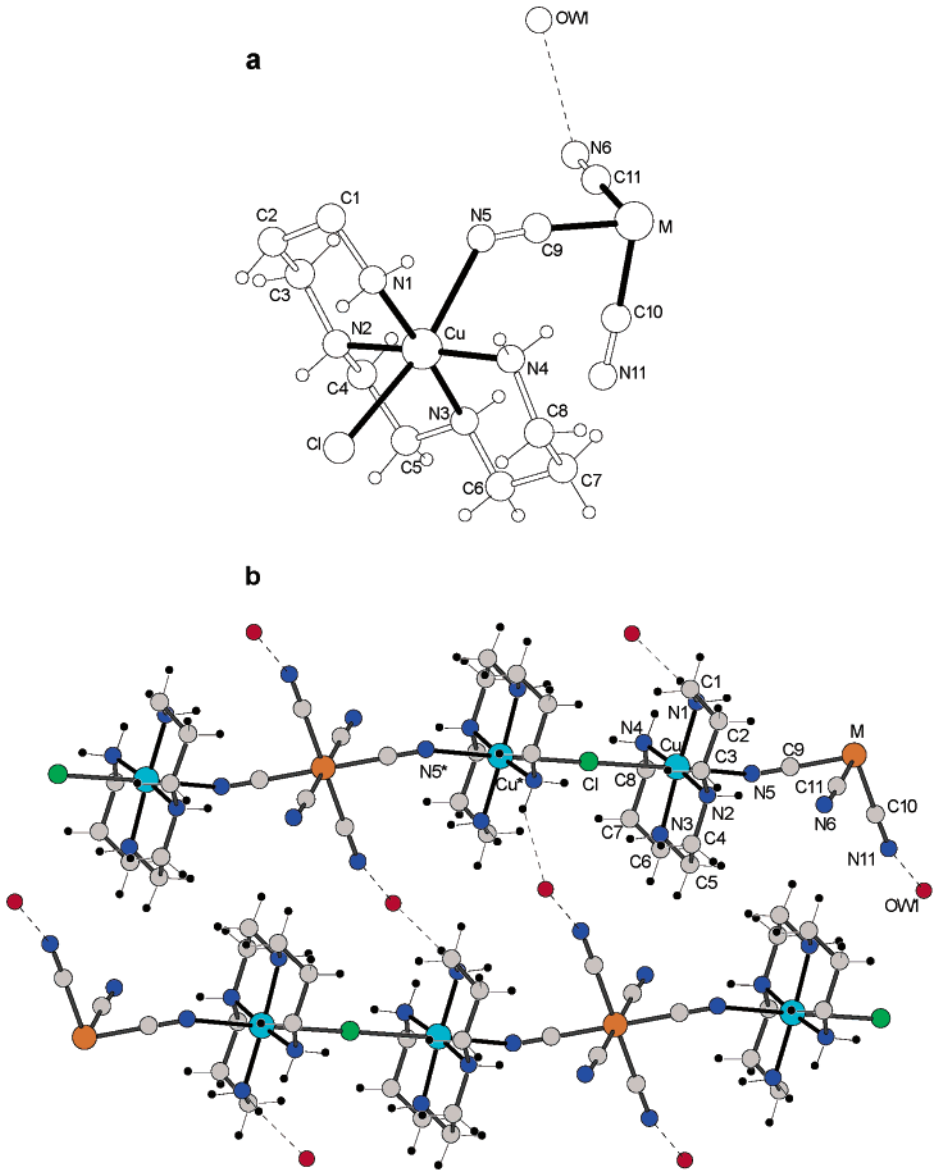

Figure 2. (a) Perspective view of the asymmetric unit of isostructural **1**, **2**, or **3** with the atom labeling scheme, where M = Co, Fe, or Cr. (b) The zigzag chains for isostructural **1**, **2**, or **3** with H-bonds between terminal cyanide and water molecule, shown by dotted lines. The C, H, N, Cl, Cu, and M (=Co, Fe, Cr) are shown by gray, black, blue, green, light blue, and orange colors, respectively. The oxygen atoms for water molecules are red.

assigned to the d−d transition of the Cu(II) chromophore.[15] The electronic spectra of **2** show intense bands at 238 and 277 nm, a relatively less intense band at 420 nm, and a weak d−d transition for the Cu(II) chromophore at 545 nm. The band at 420 nm is assigned by the spectra of $K_3[Fe(CN)_6]$ which has an intense band at 419 nm, with a weak shoulder at 500 nm. The weak shoulder is not clearly observed due to the broad nature of the Cu(II) d−d transition band at 545 nm. The spectrum for **3** is similar to that of **2** having well resolved bands at 241 and 272 nm, a moderately strong band at 375, and a d−d transition band for the Cu(II) center at 547 nm. The band at 375 nm can be explained by the sharp band at 375 nm observed in $K_3[Cr(CN)_6]$. The intense bands at ∼240 and ∼ 270 nm are commonly seen for **1**−**3**. The band near 240 nm seems to correspond to the $L_\sigma \rightarrow$ Cu charge transfer,[7] and the band at 270 nm to a band near 260 nm found for $K_3[M(CN)_6]$ (259 nm for M = Co and Fe, 261 nm for M = Cr).

Crystal Structure. The X-ray crystallography for $[(323)_2Cu_2(Cl)Co(CN)_6]_n \cdot 2n(H_2O)$ (**1**), $[(323)_2Cu_2(Cl)Fe(CN)_6]_n \cdot 2n(H_2O)$ (**2**), and $[(323)_2Cu_2(Cl)Co(CN)_6]_n \cdot 2n(H_2O)$ (**3**) proves that all three complexes are isomorphous and isostructural. A perspective view of the asymmetric unit with the atom numbering scheme of **1** is shown in Figure 2a. A useful projection of the molecular assembly of the strings is shown in Figure 2b. Selected bond distances and angles with their estimated standard deviation for **1**, **2**, and **3** are listed in Table 2.

The asymmetric unit of $[(323)_2Cu_2(Cl)Co(CN)_6]_n \cdot 2n(H_2O)$ (**1**) consists of half of a $[Co(CN)_6]^{3+}$ anion, and half of a chloride atom. The Co^{3+} ion resides at inversion centers, and the Cl atoms lie on the mirror planes. Two cyano nitrogens of $[Co(CN)_6]^{3+}$ (N5 and N5*) (* indicates a symmetry

(14) Beck, W.; Feldi, K. *Z. Anorg. Chem.* **1965**, *341*, 113.
(15) Rossoti, F. J. C. In *Modern Coordination Chemistry*; Lewis, J., Wilkins, R. G., Eds.; Interscience: New York, 1960.

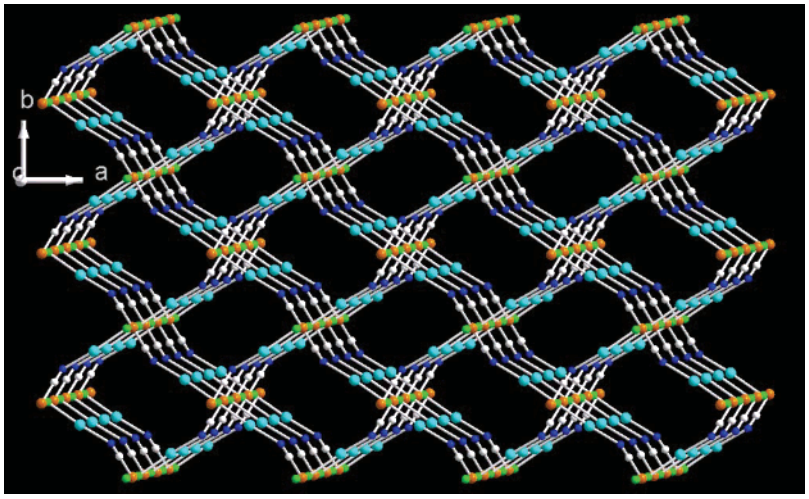

Figure 3. Inter-string array of bimetallic assemblies. The 323 ligand moiety and the terminal cyanides were omitted for clarity. The C, N, Cu, Cl, and M (=Co, Fe, Cr) are shown by gray, blue, light blue, green, and orange colors, respectively

Table 2. Selected Bond Distances and Bond Angles of **1**, **2**, and **3**

	1 (M = Co)	**2** (M = Fe)	**3** (M = Cr)
	Distances (Å)		
M−C9	1.904(6)	1.949(3)	2.080(6)
M−C10	1.886(7)	1.953(4)	2.070(5)
M−C11	1.865(7)	1.931(4)	2.074(5)
Cu−N1	2.014(5)	2.016(3)	2.012(4)
Cu−N2	2.040(5)	2.038(3)	2.046(4)
Cu−N3	2.035(5)	2.032(3)	2.030(4)
Cu−N4	2.023(5)	2.024(3)	2.025(4)
	Angles (deg)		
M−C9−N5	175.8(6)	174.0(3)	179.4(6)
M−C10−N6	176.3(6)	179.0(4)	172.2(5)
M−C11−N7	177.5(7)	176.2(3)	175.0(5)

operation, of $x, y, z \rightarrow -x, -y, -z$) are in trans positions and coordinated to the adjacent [323Cu] moiety, while the chloride atom Cl is connected to Cu1 and Cu1* (generated by the inversion operation, and a translation of 2.0, 0.0, 1.0). The atoms form 1-D zigzag chains run along the two different directions, the *a* and *b* axes. During propagation, the strings are held together by hydrogen bonding interactions to form a complicated, yet highly symmetric, 3-D network. The strings along two different directions, and the inter-string arrays, have been illustrated in Figure 3.

Owing to the Jahn−Teller effect, the copper(II) centers assume an axially distorted octahedral CuN_5Cl chromophore. The two axial positions are occupied by chloride and nitrogen atoms with distances Cu−Cl of 2.74 Å and Cu−N5 of 2.59 Å. The equatorial positions are occupied by the N_4 set of donor atoms from the 323 ligand with Cu−N distances in the range 2.01−2.04 Å. Both the cis N−Cu−N angles (84.7−92.4°) and the trans N5−Cu−Cl angle (168.73°) deviate from the ideal values of 90° and 180°, respectively. In the chain, the two CN− groups of each $[Co(CN)_6]^{3-}$ unit bridge two copper(II) atoms with a $Co^{3+}\cdots Cu^{2+}$ distance of 5.10 Å. The chloride bridged $Cu^{2+}\cdots Cu^{2+}$ distance is 5.476 Å. The Co−C9−N5, Cu−N5−C9, Cl−Cu−N5, and Cu−Cl−Cu* bond angles for the bridging cyanide and chloride groups are 175.75°, 131.67°, 168.75°, and 179.97°, respectively, which indicate that the strings adopt a zigzag disposition. The Co−C−N angles for the terminal cyanide group in $[Co(CN)_6]^{3-}$ are 176.35° and 177.48°. The cobalt centers in the $[Co(CN)_6]^{3-}$ unit adopt a minimally distorted octahedral environment; the trans C−Co−C angles are 180° whereas the cis C−Co−C are 86.40°, 88.68°, and 90.30°. The water molecule is strongly hydrogen bonded to a free cyano fragment with distances of 1.93 Å for N6···Hw1 and 2.82 Å for N6···O. The distances between the copper and axial bridging atom Cl and/or N5 are 2.74 and 2.58 Å, respectively, for **2** and 2.733 and 2.60 Å for **3**. The angles in the bridging region for compound **2** are Fe−C9−N5 = 174.00°, Cu−N5−C9 = 133.79°, Cl−Cu−N5 = 168.94°, and Cu−Cl−Cu* = 180.30° and for **3** are Cr−C9−N5 = 172.26°, Cu−N5−C9 = 131.96°, Cl−Cu−N5 = 167.44°, and Cu−Cl−Cu* = 179.80°.

The bimetallic assemblies, **1**−**3**, have essentially the same molecular and network structure. However, they show a significant difference in the average M−C bond distance, that becomes longer in the order M = Co < Fe < Cr. This order is in accord with the decreasing number of dπ electrons at the metal centers.[16] This fact suggests that the π-back-donation from the metal to the vacant CN orbital decreases in this order (see Table 2). The *a* and *b* axis lengths of **1**−**3** reflect the M−C distance and increases in the order M = Co < Fe < Cr (see Table 1).

Magnetic Properties. The thermal dependence of the $\chi_M T$ product for **1** ($\chi_M T$ is the magnetic susceptibility per Cu_2-Co) is shown in Figure 4. At room temperature, $\chi_M T$ is equal to 0.82 $cm^3\ mol^{-1}$ K, a value which is as expected for two magnetically isolated Cu(II) ions (Co(III) is diamagnetic). Upon cooling, the value of $\chi_M T$ is constant until 30 K, and then, it decreases to 0.13 $cm^3\ mol^{-1}$ K at 1.9 K. The susceptibility versus *T* plot exhibits a maximum at 3.5 K under an applied magnetic field of 500 Oe (see inset of Figure 4). All these features indicate the occurrence of weak antiferromagnetic interactions between the copper(II) ions. The exchange pathway for this antiferromagnetic coupling

(16) (a) Sharpe, A. G. *The Chemistry of Cyano Complexes of the Transition Metals*; Academic Press: London, 1976. (b) Fee, J. A. *Struct. Bonding* **1975**, *23*, 1. (c) Ryan, R. R.; Swanson, B. I. *Inorg. Chem.* **1974**, *13*, 1681.

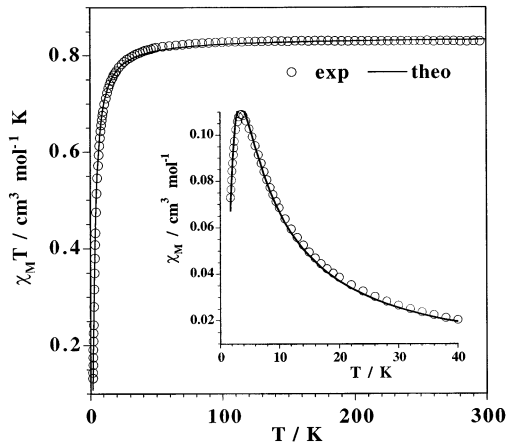

Figure 4. Thermal dependence of $\chi_M T$ for compound **1**. The inset shows the susceptibility curve: (○) experimental data; (—) best theoretical fit (see text).

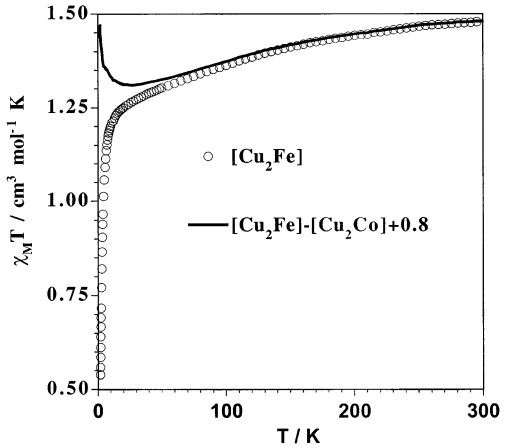

Figure 6. Thermal dependence of $\chi_M T$ for compound **2**: (○) experimental data, (—) calculated curve subtracting the antiferromagnetic interaction between Cu(II) ions (see text).

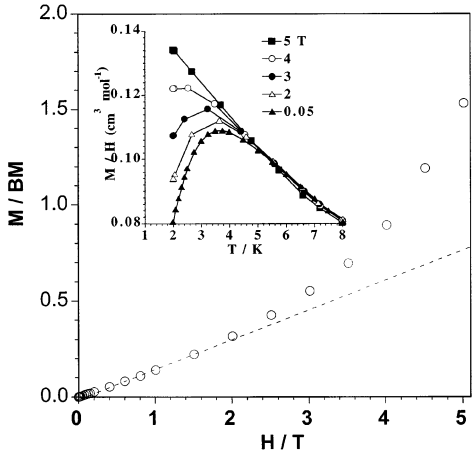

Figure 5. Field dependence of the magnetization for compound **1**. The inset shows the field dependence of the susceptibility (M/H); the solid line is a guide to the eye.

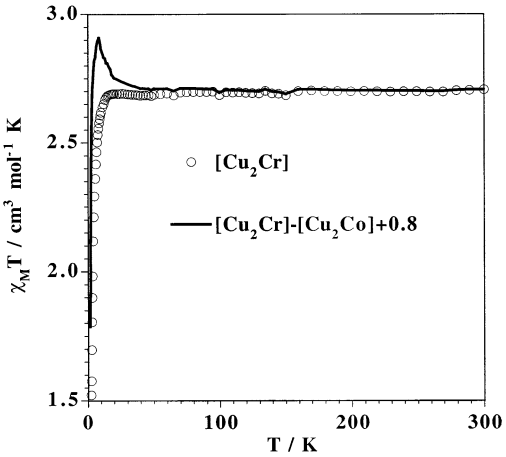

Figure 7. Thermal dependence of $\chi_M T$ for compound **3**: (○) experimental data, (—) calculated curve subtracting the antiferromagnetic interaction between Cu(II) ions (see text).

must be attributed to the single chloro bridge (Cu···Cu separation of ca. 5.48 Å), whereas that involving the N−C−Co(III)−C−N bridge is to be discarded due to the larger copper−copper separation (ca. 10 Å). Consequently, from a magnetic point of view, compound **1** behaves as a copper(II) dimer. The susceptibility data of this compound have been analyzed through a simple Bleaney−Bowers expression, the Hamiltonian being defined as $\mathbf{H} = -J\mathbf{S}_A\mathbf{S}_B$. The best-fit parameters are the following: $J = -4.0$ cm^{-1}, $g = 2.07$, and $R = 3.2 \times 10^{-5}$ (R is the agreement factor defined as $R = \sum_i[(\chi_M T)_{obs}(i) - (\chi_M T)_{calc}(i)]^2/\sum_i[(\chi_M T)_{obs}(i)]^2$).

The susceptibility maximum of this compound depends on the magnitude of the applied magnetic field (H). A broadening of this maximum is observed as long as the field is increased, and it disappears when the applied field is greater than 4 T (see inset of Figure 5). This metamagnetic behavior is also observed in the magnetization versus H plot at 1.9 K, (Figure 5) where a prominent sigmoid curve can be seen with a predicted inflection point close to 4 T. The saturation of the magnetization could not be obtained because of the maximum value of the magnetic field in our device is only 5 T. The value of the critical field, $H_c = 4$ T (Zeeman energy of ca. 4 cm^{-1}), is in agreement with the observed antiferromagnetic interaction between the copper(II) ions ($J = -4.0$ cm^{-1}). This means that values of the magnetic field larger than 4 T are able to overcome the antiferromagnetic interaction, the local spin doublets being placed in a parallel arrangement.

The thermal dependence of the $\chi_M T$ product for **2** (χ_M is the magnetic susceptibility per Cu_2Fe) is shown in Figure 6. At room temperature, $\chi_M T$ is equal to 1.48 cm^3 mol^{-1} K, a value which is as expected for two copper(II) and one low-spin iron(III) ions, magnetically isolated. Upon cooling, the value of $\chi_M T$ decreases smoothly until 15 K and then sharply to a value of 0.53 cm^3 mol^{-1} K at 1.9 K. No maximum is observed in the susceptibility versus T plot.

A similar magnetic behavior is observed for **3** (Cu_2Cr) except for the fact that the $\chi_M T$ value remains basically constant ($\chi_M T = 2.70$ cm^3 mol^{-1} K) until 15 K and then decreases abruptly to a final value of 1.52 cm^3 mol^{-1} K at 1.9 K (see Figure 7). The magnetic behavior for **2** and **3** corresponds to an overall antiferromagnetic interaction.

It is well-known that the magnetic interaction between Cu(II) and Cr(III), or low-spin Fe(III), through bridging cyanide is ferromagnetic[3b,4c−e] in nature (case of strict orthogonality between the magnetic orbitals). Because the

antiferromagnetic interaction between the copper(II) ions through single chloro bridges can mask the ferromagnetic one in the pair Cu(II)−M(III) (M = Cr and Fe), a way to visualize the expected ferromagnetic interaction consists of subtracting from the $\chi_M T$ data of **2** (the same for **3**) those of compound **1**, and further addition of a constant value of 0.8 $cm^3\ mol^{-1}$ K, corresponding to two magnetically isolated copper(II) ions with $g = 2.07$. The resulting $\chi_M T$ versus T plots correspond to the solid lines in Figures 6 and 7, which would represent the magnetic interaction in the couple Cu(II)−M(III) without the Cu(II)−Cu(II) magnetic interaction. As can be seen, the resulting curves (solid lines) clearly show a slight increase of the $\chi_M T$ values at low temperatures which would correspond to the expected ferromagnetic interaction. The presence of a minimum in the calculated $\chi_M T$ versus T plot is due to the spin−orbit coupling in the $^2T_{2g}$ ground term of the low-spin iron(III) ion.

Simple orbital considerations account for the weak magnetic interaction observed in this series of complexes. The magnetic orbital of the copper(II) ion is of the type $d_{x^2-y^2}$ [the x and y axes being roughly defined by the short Cu−N(macrocycle) bonds] with a low-spin density in the axial positions which are filled by the Cl atoms. This fact, together with the large value of the Cu−Cl distance (ca. 2.7 Å), accounts for the weakness of the magnetic coupling observed. Similarly, the weak ferromagnetic coupling between Cu(II) and M(III) is due to the great value of the axial Cu−N(cyanide) distance (2.6 Å) as well as to the significant bending of the Cu−C−N(cyanide) angle (ca. 133°).

Concluding Remarks

The selective choice of the second bridging agent, chloride, resulted in the formation of zigzag strings which are the repeated combination of a homometallic antiferromagnetic fragment of Cu−Cl−Cu and heterometallic Cu−CN−M (M = Co^{3+}, Fe^{3+}, Cr^{3+}) fragments. Furthermore, the approach may be useful to further explore the opportunity of building new materials with combinations of cyanometalates and a second bridging agent, such as pseudo-halides like azide.

The bimetallic assembly $[(323)_2Cu_2(Cl)Co(CN)_6]_n \cdot 2n(H_2O)$ (**1**) exhibits a metamagnet behavior with Neel temperature $T_N = 3.5$ K. The value of the critical field (4 T) is similar to the singlet−triplet energy gap of $-4\ cm^{-1}$, which signifies that a field higher than 4 T overrules the antiferromagnetism, and the local spin doublets remain in a parallel arrangement. Within the strings of assemblies **2** and **3**, both weakly aniferromagnetic and weak ferromagnetic interactions were observed. The overall interaction was observed to be antiferromagnetic, as the ferromagnetic contribution was masked by the antiferromagnetic contribution. The extent of weaker ferromagnetic exchange was evidenced by a combined consideration of magnetic susceptibilities experienced for **2** or **3** with **1.** The metal ions responsible for ferromagnetism in **2** and **3** were replaced by a magnetically inert Co^{3+}, in the case of **1**; otherwise, all the other factors governing the magnetic character were kept the same. The existence of the weak nature of the magnetic interactions was explained by the fact that the spin density is low along the axial position of copper atom, and by the longer axial bond lengths for copper ions and the significant extent of bending in the Cu−NC−M angle.

Acknowledgment. We thank the Robert A. Welch Foundation for support of these studies (Grant 592 to I.B.) and for postdoctoral support to Dr. Manas K. Saha. Financial support from the Spanish DGICYT through Project BQU2001-2928 and the Training and Mobility Research Program from the European Union TMR Contract ERBFMRXCT-980181 is also acknowledged.

Supporting Information Available: Crystallographic data in CIF format. This material is available free of charge via the Internet at http://pubs.acs.org.

IC034897N